Protective Effects of GLP-1 on Glomerular Endothelium and Its Inhibition by PKC Activation in Diabetes

(Article begins on next page)

Protective Effects of GLP-1 on Glomerular Endothelium and Its Inhibition by PKCβ Activation in Diabetes

Akira Mima,[1] Junko Hiraoka-Yamomoto,[1] Qian Li,[1] Munehiro Kitada,[1] Chenzhong Li,[1] Pedro Geraldes,[2] Motonobu Matsumoto,[1] Koji Mizutani,[1] Kyoungmin Park,[1] Christopher Cahill,[1] Shin-Ichi Nishikawa,[3] Christian Rask-Madsen,[1] and George L. King[1]

To characterize glucagon-like peptide (GLP)-1 signaling and its effect on renal endothelial dysfunction and glomerulopathy. We studied the expression and signaling of GLP-1 receptor (GLP-1R) on glomerular endothelial cells and the novel finding of protein kinase A–dependent phosphorylation of c-Raf at Ser259 and its inhibition of angiotensin II (Ang II) phospho–c-Raf(Ser338) and Erk1/2 phosphorylation. Mice overexpressing protein kinase C (PKC)β2 in endothelial cells (EC-PKCβ2Tg) were established. Ang II and GLP-1 actions in glomerular endothelial cells were analyzed with small interfering RNA of GLP-1R. PKCβ isoform activation induced by diabetes decreased GLP-1R expression and protective action on the renal endothelium by increasing its degradation via ubiquitination and enhancing phospho–c-Raf(Ser338) and Ang II activation of phospho-Erk1/2. EC-PKCβ2Tg mice exhibited decreased GLP-1R expression and increased phospho–c-Raf(Ser338), leading to enhanced effects of Ang II. Diabetic EC-PKCβ2Tg mice exhibited greater loss of endothelial GLP-1R expression and exendin-4–protective actions and exhibited more albuminuria and mesangial expansion than diabetic controls. These results showed that the renal protective effects of GLP-1 were mediated via the inhibition of Ang II actions on cRaf (Ser259) and diminished by diabetes because of PKCβ activation and the increased degradation of GLP-1R in the glomerular endothelial cells. *Diabetes* 61:2967–2979, 2012

Endothelial pathologies such as thrombotic microangiopathy and mesangiolysis are parts of glomerulopathy because of insulin resistance and diabetes, which are leading causes of clinical renal disease (1,2). Endothelial dysfunction is postulated to accelerate the progression of diabetic glomerulopathy as a result of the inhibition of endothelial nitric oxide (NO) synthesis (eNOS) and its product, NO (3).

We have reported that activation of the β isoform of protein kinase C (PKC) by hyperglycemia can cause glomerular endothelial dysfunction and reduce eNOS activation partially owing to inhibition of insulin action on glomerular endothelial cells (4,5). Clinically, ruboxistaurin (RBX), a specific inhibitor of PKCβ, has been reported to improve endothelial dysfunction induced by hyperglycemia (4,6). Further, studies have associated PKCβ activation with glomerular pathology induced by hyperglycemia possibly due to the enhancement of angiotensin action (7). However, the biochemical mechanism by which PKCβ enhances angiotensin II (Ang II) action to accelerate the progression of diabetic glomerulopathy has not been clarified.

Recently, glucagon-like peptide-1 (GLP-1) has been reported to biologically improve endothelial function and prevent some renal pathologies in diabetic rodents (8,9). However, a mechanistic explanation regarding GLP-1–protective action on the endothelial cell is unknown.

GLP-1 is a gut incretin hormone that augments glucose-dependent insulin responses in the β cells (10). GLP-1 receptor (GLP-1R) is present abundantly in the gastrointestinal tract but has also been reported in endothelium and kidney and may stimulate NO production (8,11,12). In this study, we have identified a new biochemical mechanism for GLP-1 to inhibit Ang II inflammatory action via the c-Raf/extracellular signal–related kinase (Erk)1/2/plasminogen activator inhibitor (PAI)-1 pathway in glomerular endothelial cells. Further, we have demonstrated a dual signaling mechanism by which diabetes, via PKCβ activation, can increase Ang II action by increasing the inflammatory cytokines and extracellular matrix and inhibiting GLP-1–protective effects by reducing GLP-1R expression in the glomerular endothelium.

RESEARCH DESIGN AND METHODS

Generation of endothelial cell–specific *PKCβ2*–overexpressing mice. All animal protocols were approved by the Joslin Diabetes Center committee in accordance with NIH guidelines. The *pVECD-PKCβ2* vector was constructed by inserting mouse *PKCβ2* cDNA into *pVECD* vector (13). Transgenic mice expressing PKCβ2 were generated from C57BL/6J mice. Diabetes was induced by five consecutive days of injections of streptozotocin (STZ) (55 mg/kg body wt; Sigma) in 0.05 mol/L citrate buffer (pH 4.5). Blood glucose levels were determined by glucose analyzer (Yellow Spring Instruments). Glycemic levels >16.7mmol/L were defined as having diabetes. Two weeks after diabetes, exendin-4 (1.0 nmol/kg/day; Sigma) or diluents were administrated intraperitoneally to mice for 6 months. Regular human insulin (10 mU/g; Lilly) or diluents were injected into the inferior vena cava for 10 min to study insulin signaling. Kidneys were harvested and procedures were performed within 30 min.
Measurement of blood pressure. Blood pressure was determined in conscious animals using a noninvasive computerized automated tail-cuff system (Vistech Systems). After the mice were trained for five consecutive days, they were placed on a heated platform and studied for three 10-cycle measurements.
Measurement of urinary albumin, creatinine, and cAMP. Urinary albumin was measured from 24-h urine collection with mice housed in individual metabolic cages and assessed by Albuwell (Exocell). Creatinine levels were measured by colorimetric detection kit (Assay Designs), and urinary cAMP was measured after injection with exendin-4 or vehicle by using ELISA kit (Cell Biolab).
Isolation of glomeruli and cell culture. Isolation of mouse glomeruli was performed as previously described (14). Rat glomerular and lung endothelial cell were also cultured as previously described (4).
Immunoblot analysis. Samples were dissolved in 0.5% Nonidet P-40 and immunoprecipitated with antibody to GLP-1R (Santa Cruz Biotechnology) and

protein A/G-Sepharose beads. The proteins were separated by SDS-PAGE and subsequently blotted with antibodies as indicated.

Immunohistochemistry and real-time PCR analysis. Immunohistochemistry and its analysis were performed as previously described (4). Real-time PCR was also performed as previously described (4) (Supplementary Table 1).

Data analysis. Data are expressed as means ± SD. Comparisons were made between groups using either two-sample and paired t tests for two-way comparisons or one-way ANOVA for multiple groups to establish statistically significant differences. All analyses were performed using StatView (SAS Institute). Statistical significance was defined as $P < 0.05$.

RESULTS

Effect of diabetes and PKCβ2 activation on GLP-1R expression. Double immunostaining studies showed that GLP-1R was mainly expressed by glomerular endothelial cells and that expression levels were decreased by 43 ± 12% in diabetic mice compared with nondiabetic mice (Fig. 1A). Immunoblot study of renal cortex lysate showed that GLP-1R protein expression was decreased by 35 ± 9% after 6 months of diabetes (Fig. 1B). In the glomeruli, GLP-1R protein expression was decreased by 37 ± 7% (Supplementary Fig. 1) after 3 months of diabetes. In contrast, GLP-1R mRNA expression was not changed by diabetes (Fig. 1C). To evaluate the mechanisms of insulin receptor substrate 1 diabetes-inhibitory actions, we studied the effect of PKC activation on GLP-1R expression in glomerular endothelial cells (RGECs). PKC activation by phorbol 12-myristate 13-acetate (PMA) decreased protein expression of GLP-1R by 46 ± 4% (Fig. 1D) without altering GLP-1R mRNA levels (Fig. 1E). Addition of GF109203X (GFX), a general PKC inhibitor, and RBX reversed the inhibitory effect of PMA by 29 ± 8 and 17 ± 7%, respectively. Since diabetes and PKC activation appear to affect GLP-1R by a posttranscriptional mechanism, the addition of proteasome inhibitor MG132 in RGECs increased GLP-1R protein levels by 29 ± 10% during PMA treatment (Fig. 1D). To confirm that increases in the degradation of GLP-1R were induced by PKC activation, RGECs were exposed to 100 nmol/L PMA for 4 h, which increased the ubiquitinated GLP-1R levels significantly by 8.9 ± 1.1-fold; levels were inhibited by GFX or RBX by 37 ± 6 and 22 ± 6%, respectively (Fig. 1F). Adenovirus-mediated overexpression of PKCβ2 (Ad-PKCβ2) in RGECs decreased GLP-1R protein levels by 29 ± 3% compared with a control construct (Fig. 1G) without changing mRNA expression (Fig. 1H). Overexpression of PKCα and PKCδ isoforms by infection with Ad-PKCα and Ad-PKCδ did not decrease GLP-1R protein expression (Fig. 1G).

To determine whether PKCβ2 activation in the endothelial cells can decrease the expression of GLP-1R, we created mice overexpressing mouse PKCβ2 in endothelial cells (EC-PKCβ2Tg) using a transgene consisting of a fragment of the vascular endothelial-cadherin promoter and mouse PKCβ2 cDNA (Supplementary Fig. 2A). Transgenic founder lines carrying the mouse PKCβ2 transgene were identified by Southern blot analysis (Supplementary Fig. 2B). In situ PKC activity increased by 53 ± 16% in the glomeruli of EC-PKCβ2Tg mice (Supplementary Fig. 2C). RT-PCR analysis for PKCβ2 revealed that mRNA expression of the transgene in the glomeruli increased by 32 ± 8-fold compared with wild-type (WT) mice (Supplementary Fig. 2D). Immunoblot analyses showed that expression of PKCβ2 in cytosolic and membrane fractions from glomeruli increased by 2.8 ± 0.3- and 7.5 ± 0.3-fold, respectively, in EC-PKCβ2Tg compared with WT controls (Supplementary Fig. 2E). In contrast, the levels of PKCα, PKCδ, and PKCε were not changed in cytosolic or

membrane fractions in the renal cortex of transgenic mice (Supplementary Fig. 2F). Immunoblot analyses of primary lung endothelial cells showed that the expression of PKCβ increased by 2.6 ± 0.9-fold greater in transgenic than in WT mice (Supplementary Fig. 2G). Double immunostaining of the renal glomeruli showed that the increases of PKCβ2 were detected mainly in the glomerular endothelial cells (Supplementary Fig. 2H).

GLP-1R expression in the renal glomeruli, measured by immunohistochemistry, was reduced by 45 ± 19% in the EC-PKCβ2Tg mice versus WT mice. After 6 months of diabetes, GLP-1R expression in diabetic EC-PKCβ2Tg mice was reduced by 64 ± 19% compared with nondiabetic WT mice and by 37 ± 14% versus diabetic WT mice (Fig. 2A). Immunoblot analysis showed that GLP-1R protein expression decreased in nondiabetic and diabetic EC-PKCβ2Tg mice by 35 ± 4 and 51 ± 3%, respectively, compared with nondiabetic WT mice and reduced by 22 ± 3% when diabetic EC-PKCβ2Tg mice were compared with diabetic WT mice (Fig. 2B). GLP-1R protein expression also decreased in glomeruli of nondiabetic and diabetic EC-PKCβ2Tg mice by 34 ± 7 and 59 ± 6%, respectively, compared with nondiabetic WT mice and reduced by 34 ± 10% when diabetic EC-PKCβ2Tg mice were compared with diabetic WT mice (Supplementary Fig. 2I). No changes in GLP-1R mRNA expression levels were observed in any group (Fig. 2C). The levels of polyubiquitination of GLP-1R were increased significantly in diabetic WT mice by 6.5 ± 1.4-fold and in nondiabetic EC-PKCβ2Tg mice by 5.3 ± 1.1-fold compared with nondiabetic WT mice. Further, polyubiquitination of GLP-1R in diabetic EC-PKCβ2Tg mice was more prominent by 8.4 ± 1.0-fold versus nondiabetic WT mice and by 1.3 ± 0.1-fold compared with nondiabetic EC-PKCβ2Tg mice (Fig. 2D).

Nuclear factor-κB activation and inflammation in renal cortex. We also characterized the effect of PKCβ2 activation on nuclear factor-κB (NF-κB) and inflammatory cytokine expression, which are markers of diabetic glomerulopathy and angiotensin activation (15,16). NF-κB activation was observed to be 1.3 ± 0.3-fold higher in the renal cortex of EC-PKCβ2Tg mice than in diabetic WT mice after 6 months of diabetes (Supplementary Fig. 3A). Similarly, NF-κB, as measured by DNA binding, increased in both diabetic EC-PKCβ2Tg and WT mice compared with their nondiabetic controls after 3 and 6 months of diabetes (by 1.3 ± 0.1-fold in WT and by 1.5 ± 0.2-fold in EC-PKCβ2Tg mice, respectively) (Supplementary Fig. 3B). For inflammatory cytokines, expression of tumor necrosis factor-α mRNA levels was increased by 3.2 ± 1.1- and 1.4 ± 0.2-fold after 3 and 6 months of diabetes in diabetic versus nondiabetic WT mice. After 6 months of diabetes, tumor necrosis factor-α mRNA levels were 1.4 ± 0.2-fold higher in EC-PKCβ2Tg mice compared with WT mice (Supplementary Fig. 3C). Similarly, expression of interleukin-6 mRNA levels in the renal cortex of diabetic WT mice was increased by 2.9 ± 0.6- and 2.0 ± 0.5-fold after 3 and 6 months of diabetes compared with WT mice. For EC-PKCβ2Tg mice, diabetes increased interleukin-6 mRNA expression by 1.5 ± 0.5-fold compared with diabetic WT mice after 6 months of diabetes (Supplementary Fig. 3D). Diabetes also increased the expression of CD68 mRNA levels in WT mice by 6.1 ± 2.9-fold and in EC-PKCβ2Tg mice by 6.1 ± 2.8-fold at 3 months (Supplementary Fig. 3E).

Effect of diabetes on renal function and pathology. After 6 months, body weight, blood glucose, and plasma insulin concentrations were not different between diabetic
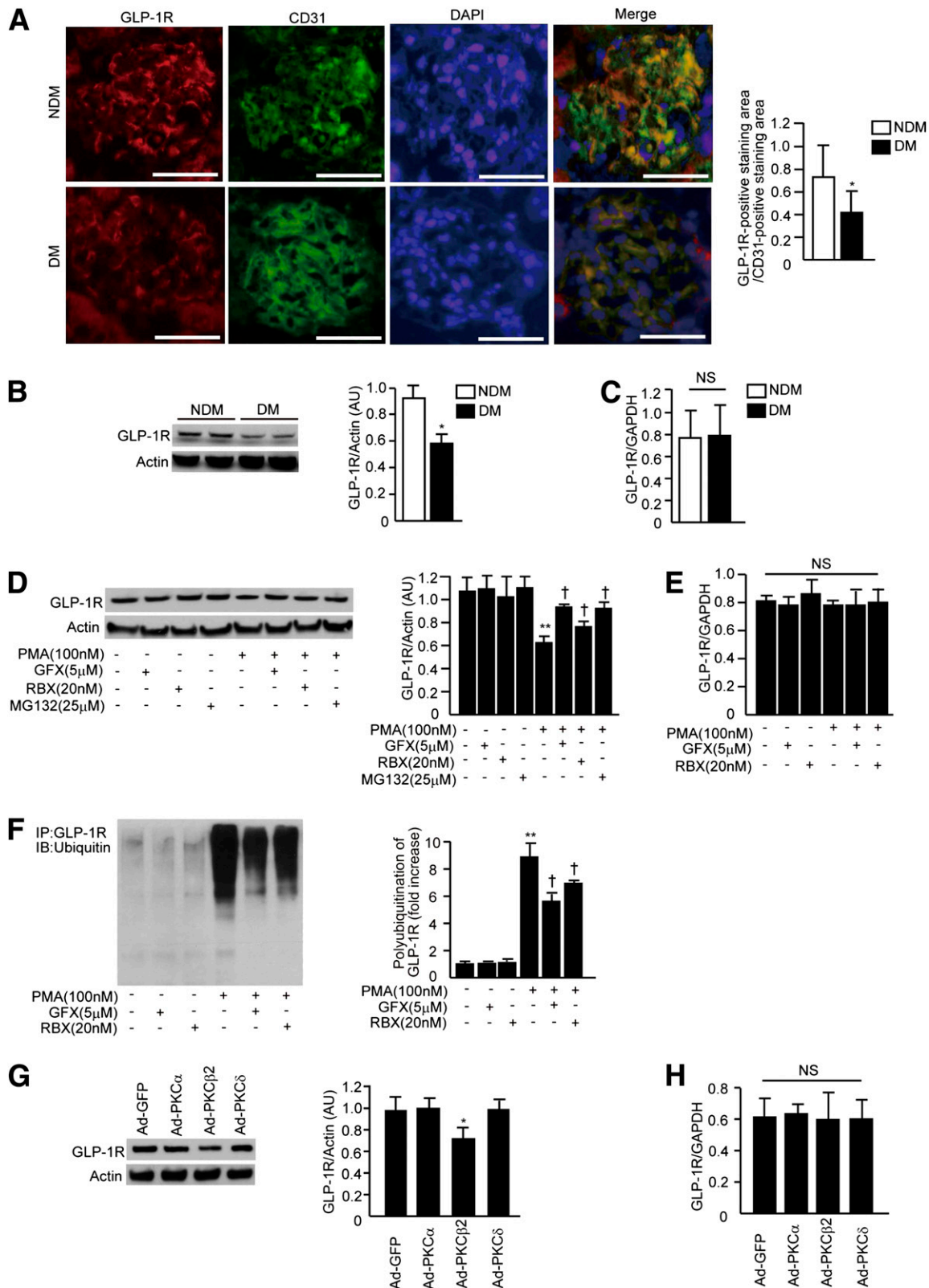
FIG. 1. Diabetes and PKCβ2 activation decreases GLP-1R. *A*: Immunostaining for GLP-1R and CD31 and merge images in the glomeruli and morphometric analysis of glomerular expression of GLP-1R and CD31. For quantification of the expression of GLP-1R and CD31, the positive staining area/glomerular area (%) was measured using ImageJ (NIH). For each animal, 50 glomeruli were evaluated. Bar = 50 μm. n = 6 in non-diabetic WT and diabetic WT mice; n = 7 in nondiabetic transgenic and diabetic transgenic mice. n = number of mice. DM, mice with STZ-induced diabetes; NDM, nondiabetic mice. *P < 0.05. Magnification ×400. *B*: Immunoblots of GLP-1R from renal cortex of mice with STZ-induced diabetes for 6 months. n = 6 in nondiabetic WT and diabetic WT mice; n = 7 in nondiabetic transgenic and diabetic transgenic mice. *P < 0.05. *C*: GLP-1R mRNA expression in the renal cortex of mice with STZ-induced diabetes for 6 months. n = 6 in nondiabetic WT and diabetic WT mice; n = 7 in nondiabetic transgenic and diabetic transgenic mice. *D*: Immunoblots of GLP-1R in RGECs. RGECs were incubated with PMA (4 h) with or without a PKC-specific inhibitor (GFX), PKCβ-specific inhibitor (RBX), or proteasome inhibitor (MG132). **P < 0.001 vs. PMA⁻, GFX⁻, RBX⁻, and

EC-PKCβ2Tg and WT mice or between nondiabetic EC-PKCβ2Tg and WT mice (Table 1 and Supplementary Table 2). Diabetic EC-PKCβ2Tg mice exhibited more albuminuria compared with diabetic WT mice by 1.5 ± 0.5-fold (Fig. 3A), but they did not differ in creatinine clearance and glomerular filtration rates (Supplementary Figs. 3F and G). The width of glomerular basement membrane (GBM) was significantly increased by 1.3 ± 0.4-fold in diabetic EC-PKCβ2Tg mice compared with diabetic WT littermates of the same age (Fig. 3B). Mesangial matrix expansion was 1.4 ± 0.4-fold greater in diabetic EC-PKCβ2Tg mice than in diabetic WT mice. Diabetic EC-PKCβ2Tg mice also exhibited a greater fraction of glomerular area stained for type IV collagen (Col4) and fibronectin than diabetic WT mice (1.3 ± 0.3- and 1.8 ± 0.5-fold higher, respectively) (Fig. 3C). Protein expression of Col4 and fibronectin in the renal cortex were increased significantly in both groups of diabetic mice, but the increases were much greater in diabetic EC-PKCβ2Tg mice by 1.4 ± 0.1-fold compared with diabetic WT mice (Supplementary Fig. 3H). This was also reflected in their mRNA levels (Supplementary Fig. I).

Evaluation of PAI-1, tissue plasminogen activator, and eNOS activation in EC-PKCβ2Tg mice. In immunohistochemistry studies, diabetes increased PAI-1–positive areas in the glomeruli of diabetic EC-PKCβ2Tg mice by 1.3 ± 0.4-fold more than in diabetic WT mice (17) (Fig. 3D). Expression of PAI-1 mRNA level was also increased in the renal cortex of both diabetic WT mice and EC-PKCβ2Tg mice in concordance with histological studies (Supplementary Fig. 3J). In contrast, areas positive for tissue plasminogen activator and its mRNA did not change in EC-PKCβ2Tg or WT mice compared with nondiabetic controls (Supplementary Figs. 3K and J).

Analysis of eNOS expression and activation in the renal cortex showed that insulin increased both phospho-Akt and phospho-eNOS significantly in WT mice, but its effect was decreased in EC-PKCβ2Tg mice compared with WT mice by 63 ± 8 and by $72 \pm 7\%$, respectively ($P < 0.05$) (Supplementary Fig. 3L) (3).

Effect of exendin-4 in diabetic EC-PKCβ2Tg mice. To determine whether GLP-1 can prevent endothelial dysfunction induced by diabetes, we determined the effect of treatment with exendin-4, an analog of GLP-1. Infusion with exendin-4 significantly increased urinary cAMP in nondiabetic WT mice by 1.9 ± 0.6-fold, which was decreased by $29 \pm 13\%$ in diabetic WT mice and by $28 \pm 12\%$ in nondiabetic EC-PKCβ2Tg mice. Exendin-4 did not significantly increase urinary cAMP in diabetic EC-PKCβ2Tg mice (Fig. 4A). Treatment with exendin-4 did not prevent the reduction of GLP-1R protein (Supplementary Fig. 4A) or mRNA levels (Supplementary Fig. 4B) in the renal cortex or affect body weight, blood glucose, blood pressure, urine volume, food intake, plasma insulin, or creatinine clearance (Supplementary Table 2 and Supplementary Fig. 4C). In contrast, exendin-4 significantly decreased albuminuria in both diabetic WT and EC-PKCβ2Tg mice by 27 ± 10 and

$44 \pm 20\%$, respectively (Fig. 4B). Quantitative analysis of immunohistochemistry showed that exendin-4 treatment reduced mesangial matrix fraction in both diabetic WT and EC-PKCβ2Tg mice by 38 ± 10 and $31 \pm 8\%$, respectively (Fig. 4C and Supplementary Fig. 4D). Col4- and fibronectin-positive staining areas were reduced by exendin-4 treatment (Col4 by $26 \pm 8\%$ in diabetic WT mice and $27 \pm 9\%$ in diabetic EC-PKCβ2Tg mice and fibronectin by $26 \pm 11\%$ in diabetic WT mice and $29 \pm 13\%$ in diabetic EC-PKCβ2 Tg mice, respectively) (Supplementary Fig. 4D). Similar reductions in the mRNA were observed when EC-PKCβ2Tg mice were treated with exendin-4 (Supplementary Fig. 5A).

Immunostaining analysis showed that exendin-4 decreased diabetes-induced elevation of PAI-1 protein expression in diabetic WT and EC-PKCβ2Tg mice (by 32 ± 11 and $31 \pm 10\%$, respectively) (Fig. 4D and Supplementary Fig. 5B). Expression of PAI-1 mRNA in renal cortex was decreased by exendin-4 treatment both in diabetic WT and EC-PKCβ2Tg mice by 24 ± 9 and $32 \pm 10\%$, respectively (Supplementary Fig. 5C).

Exendin-4 decreased mRNA expression of macrophage markers CD68 and CXCL2 in diabetic WT (CD68 by 52 ± 7 and $31 \pm 10\%$, respectively) (Supplementary Fig. 5D) and EC-PKCβ2Tg (CXCL2 by 36 ± 11 and $35 \pm 14\%$, respectively) mice (Supplementary Fig. 5D and E) (9).

Exendin-4–mediated inhibition of c-Raf/Erk1/2/PAI-1 pathway by angiotensin II. Activation of c-Raf–Erk1/2 pathways by Ang II can mediate the expression of renal inflammatory cytokines (18–20). In RGECs, Ang II significantly increased phospho–c-Raf(Ser338), phospho-Erk1/2, and PAI-1 expression by 9.9 ± 2.4-, 9.2 ± 2.2-, and 2.2 ± 0.6-fold, respectively. Exendin-4 increased phospho–c-Raf (Ser259) significantly by 13 ± 1-fold and decreased Ang II effects on phospho–c-Raf(Ser338), phospho-Erk1/2, and PAI-1 by 37 ± 2, 52 ± 6, and $22 \pm 2\%$, respectively. H89, a selective protein kinase A inhibitor, decreased the effect of exendin-4 on phospho–c-Raf(Ser259) by $43 \pm 5\%$ and reduced exendin-4–inhibitory effects on Ang II-induced phospho–c-Raf(Ser338), phospho-Erk1/2, and PAI-1 by 38 ± 4, 35 ± 3, and $11 \pm 2\%$, respectively. mitogen-activated protein kinase kinase inhibitor PD98059 decreased Ang II action on phospho-Erk1/2 and PAI-1 by 85 ± 22 and $38 \pm 4\%$, respectively, yet it did not affect Ang II action on phospho–c-Raf(Ser338), but p38 mitogen-activated protein kinase inhibitor SB203580 did not have any effect on these markers (Fig. 5A and Supplementary Fig. 6A). However, MDL12330A, a cAMP-selective inhibitor in RGECs, reduced exendin-4–induced phospho–c-Raf(Ser259) by $68 \pm 7\%$ (Fig. 5B) and partially reduced exendin-4–inhibitory effects on Ang II action [phospho–c-Raf(Ser338), phospho-Erk1/2, and PAI-1 by 23 ± 7, 45 ± 14, and $29 \pm 9\%$, respectively] (Fig. 5B and Supplementary Fig. 6B). These results strongly suggest that GLP-1–protective action on endothelial cells is due to cAMP-induced phosphorylation of c-Raf(Ser259), which inhibits Ang II activation of phospho–c-Raf (Ser338).
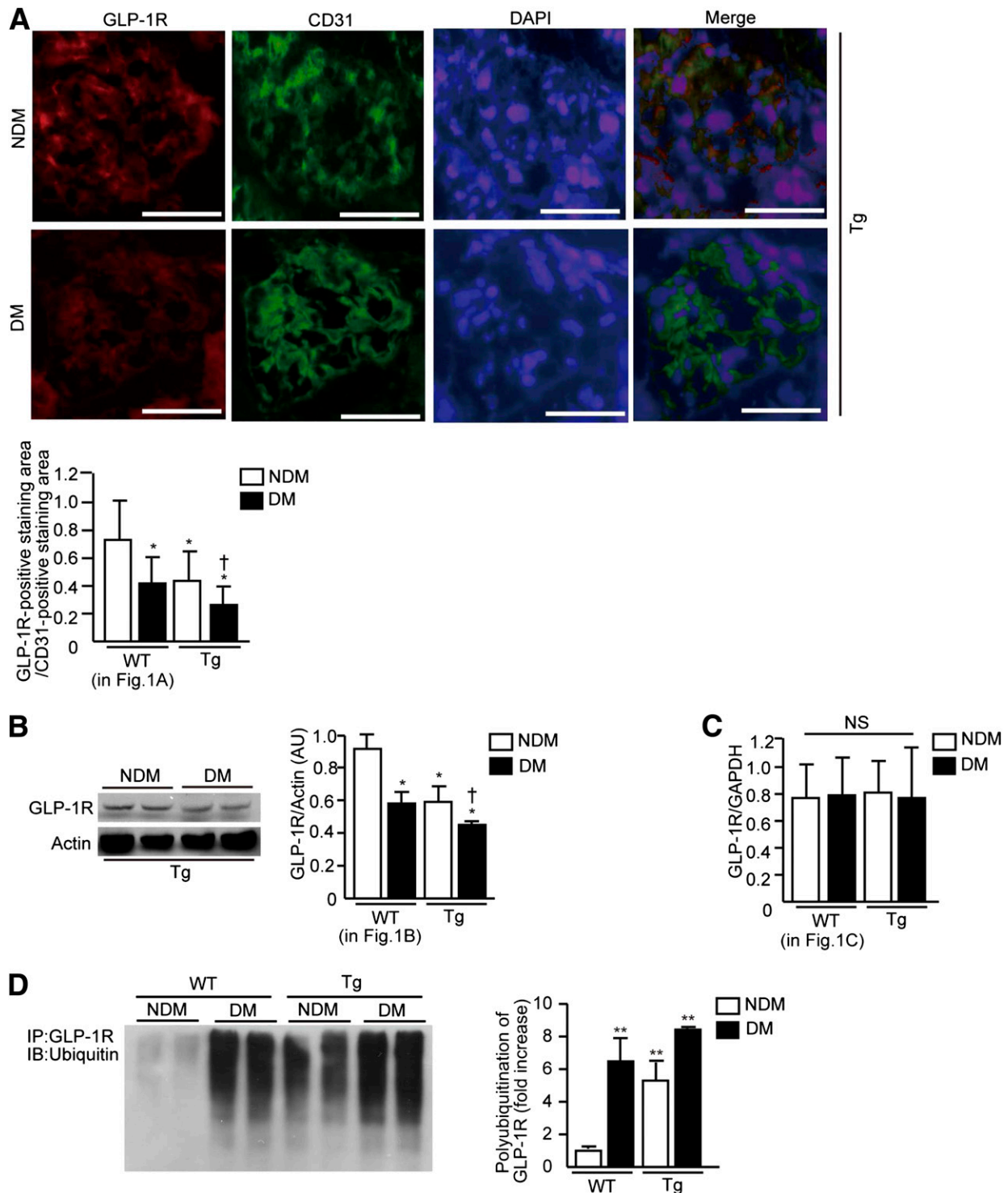

FIG. 2. Decreases of GLP-1R in the glomeruli of EC-PKCβ2Tg mice. *A*: Immunostaining for GLP-1R and CD31, merge images in the glomeruli, and morphometric analysis of glomerular expression of GLP-1R and CD31. Bar = 50 μm. DM, mice with STZ-induced diabetes; NDM, nondiabetic mice; Tg, EC-PKCβ2Tg mice. *n* = 6 in nondiabetic WT and diabetic WT mice; *n* = 7 in nondiabetic transgenic and diabetic transgenic mice. *$P < 0.05$ vs. nondiabetic WT mice. †$P < 0.05$ vs. diabetic WT mice. Magnification ×400. *B*: Immunoblots of GLP-1R from renal cortex of mice with STZ-induced diabetes for 6 months. *n* = 6 in nondiabetic WT and diabetic WT mice; *n* = 7 in nondiabetic transgenic and diabetic transgenic mice. *$P < 0.05$ vs. nondiabetic WT mice. †$P < 0.05$ vs. diabetic WT mice. *C*: GLP-1R mRNA expression in the renal cortex of mice with STZ-induced diabetes for 6 months. *n* = 6 in nondiabetic WT and diabetic WT mice; *n* = 7 in nondiabetic transgenic and diabetic transgenic mice. *D*: Immunoprecipitation and immunoblots of ubiquitin-targeted GLP-1R in each group of mice. *n* = 6 in nondiabetic WT and diabetic WT mice; *n* = 7 in nondiabetic transgenic and diabetic transgenic mice. **$P < 0.001$ vs. nondiabetic WT mice. Results are expressed as means ± SD. One of three independently performed experiments is shown. Comparisons were made between groups using either two-sample and paired *t* tests for two-way comparisons or one-way ANOVA for multiple groups to establish statistically significant differences. AU, arbitrary units; NS, not significant; IP, immunoprecipitation; IB, immunoblot. (A high-quality digital representation of this figure is available in the online issue.)

TABLE 1
Physiological characteristics of nondiabetic and diabetic WT and EC-PKCβ2Tg mice

	Nondiabetic WT	Diabetic WT	Nondiabetic Tg	Diabetic Tg
n	6	6	7	7
Body weight (g)	33.5 ± 1.3	25.2 ± 1.4*	31.9 ± 1.3	23.5 ± 3.0*
Blood glucose (mg/dL)	109 ± 8	510 ± 54*	101 ± 7	507 ± 57*
SBP (mmHg)	99.9 ± 7.8	102.8 ± 8.0	101.6 ± 10	103.4 ± 8.5
rKW/BW (mg/g)	5.2 ± 0.8	9.4 ± 1.3*	5.0 ± 0.7	11.2 ± 2.6*

Data are means ± SD unless otherwise indicated. rKW/BW, right kidney weight/ body weight; SBP, systolic blood pressure; Tg, EC-PKCβ2Tg mice. *$P < 0.05$ vs. nondiabetic WT mice.

Effect of PKC activation on c-Raf, mitogen-activated protein kinase, and PAI-1 activity. PKC activation by PMA increased phospho–c-Raf(Ser338) and phospho-Erk1/2 in RGECs by 2.7 ± 0.7- and 7.0 ± 3.3-fold, respectively, but did not alter phospho–c-Raf(Ser259). In contrast, the addition of exendin-4 increased phospho–c-Raf(Ser259) by 8.9 ± 1.0-fold in parallel with decreasing PMA-induced phospho–c-Raf(Ser338) and phospho-Erk1/2 by 58 ± 8 and 43 ± 5%, respectively (Fig. 6A). Addition of GFX or RBX decreased PMA-induced phospho–c-Raf(Ser338) by 55 ± 4 and 34 ± 4% and phospho-Erk1/2 by 53 ± 2 and 31 ± 8%, respectively (Fig. 6B). Similar to PMA, Ang II also increased phospho–c-Raf(Ser338) and phospho-Erk1/2 by 6.0 ± 2.1- and 10 ± 2-fold, respectively, which were reduced significantly by inhibitors GFX and RBX by 43 ± 2 and 26 ± 7%, respectively (Fig. 6C). Lastly, Ang II increased mRNA levels of PAI-1 by 5.4 ± 2.4-fold, which was also inhibited by GFX and RBX by 45 ± 21 and 36 ± 15%, respectively (Supplementary Fig. 6C).

Role of GLP-1R on exendin-4 and Ang II signaling. For ascertainment of whether GLP-1R was mediating exendin-4–inhibitory effect, the expression of GLP-1R was reduced by GLP-1R small interfering RNA in RGECs. The addition of GLP-1R small interfering RNA in RGECs reduced its expression by 55 ± 22% (Supplementary Fig. 6D), inhibited exendin-4–induced phospho–c-Raf(Ser259) by 47 ± 8% (Fig. 6D), and decreased exendin-4–inhibitory effects on Ang II signaling of phospho–c-Raf(Ser338), phospho-Erk1/2, and PAI-1 mRNA by 47 ± 6, 16 ± 5, and 18 ± 3%, respectively (Fig. 6D and Supplementary Fig. 6E and F). Ang II induced production of PAI-1 by 2.3 ± 0.4-fold; production was decreased by exendin-4. In contrast, knockdown of GLP-1R in RGECs reduced exendin-4–inhibitory effects by 23 ± 5% (Supplementary Fig. 6G). Lastly, blocking GLP-1R with exendin-3, a GLP-1R antagonist, inhibited exendin-4–induced phospho–c-Raf(Ser259) by 57 ± 4% and increased phospho–c-Raf(Ser338) and phospho-Erk1/2 by 35 ± 3 and 56 ± 2%, respectively (Fig. 6E and Supplementary Fig. 6H) in the presence of Ang II and exendin-4.

Evaluation of Ang II and effect of GLP-1 on c-Raf in the glomeruli. Intravenous infusing of Ang II (100 ng/kg/min) increased phospho–c-Raf(Ser338) and phospho-Erk1/2 by 8.1 ± 0.8- and 6.8 ± 0.6-fold, respectively, in the glomeruli of WT mice compared with saline infusion. Further, Ang II increased phospho-Erk1/2 significantly more in the EC-PKCβ2Tg mice than WT mice by 1.4 ± 0.2-fold. In both WT and EC-PKCβ2Tg mice, treatment with exendin-4 increased phospho–c-Raf(Ser259) by 8.6 ± 0.2- and 8.8 ± 1.0-fold, respectively, and decreased Ang II-induced phospho–c-Raf(Ser338) by 41 ± 11% in WT mice and by 31 ± 9% in EC-PKCβ2Tg mice (Fig. 7A).

Similar to the results in the glomeruli, infusing Ang II increased phospho–c-Raf(Ser338) (by 6.4 ± 0.2-fold), phospho-Erk1/2 (by 7.9 ± 3.1-fold), and PAI-1 mRNA (by 11 ± 2-fold) levels in the renal cortex compared with levels in the renal cortex of WT mice without Ang II. Further, Ang II increased phospho–c-Raf(Ser338), phospho-Erk1/2, and PAI-1 expression significantly more in the EC-PKCβ2Tg mice compared with WT mice with Ang II (by 1.3 ± 0.1-, 1.4 ± 0.1-, and 1.5 ± 0.2-fold, respectively) (Supplementary Fig. 7A and B). In both WT and EC-PKCβ2Tg mice, treatment with exendin-4 increased phospho–c-Raf(Ser259) and significantly decreased Ang II–induced phospho–c-Raf (Ser338), phospho-Erk1/2, and PAI-1 expression (Supplementary Fig. 7A and B).

As previously reported (4,21), diabetes increased phospho-Erk1/2 in the renal cortex of both WT and EC-PKCβ2Tg mice, and this increase was 1.8 ± 0.3-fold greater in diabetic EC-PKCβ2Tg mice than diabetic WT mice. Diabetes also increased phospho–c-Raf(Ser338) in the renal cortex of diabetic EC-PKCβ2Tg mice, and this increase was 1.4 ± 0.1-fold greater than the increase in diabetic WT mice. Lastly, exendin-4 treatment decreased diabetes-induced increases of phospho-Erk1/2 by 37 ± 10% and phospho–c-Raf(Ser338) by 25 ± 3% in WT mice and by 20 ± 9 and 16 ± 4% in EC-PKCβ2Tg mice (Fig. 7B).

DISCUSSION

The current study provides a biochemical pathway by which GLP-1 mediates its protective action in the glomerular endothelial cells to inhibit Ang II signaling and its proinflammatory action. These data demonstrate that hyperglycemia via the activation of PKCβ can cause endothelial dysfunction through a dual pathway including reduction of GLP-1R and enhancement of Ang II signaling and action.

Previously, GLP-1R activation by exendin-4 was shown to inhibit Ang II activation in renal proximal tubular cells (22). Our results demonstrate that GLP-1 is partly mediating its protective action via its own receptor by the activation of PKA. The elevation of cAMP levels increased phospho–c-Raf(Ser259), which may inhibit phospho–c-Raf (Ser338)/phospho-Erk1/2, which are activated by Ang II to induce its inflammatory action such as PAI-1 expression. Several studies have shown that phosphorylation of c-Raf (Ser259) induced by cAMP can inhibit the action of phospho–c-Raf(Ser338), leading to inflammatory action (23,24). The inhibitory effect of cAMP is likely to be direct, since Dhillon et al. (24) and others have reported a direct interaction between PKA and c-Raf (25–26). We have shown for the first time in vivo that GLP-1 only increased Ser259 phosphorylation and Ang II–increasing Ser338 phosphorylation on c-Raf in renal glomeruli. However, when the two were infused together, GLP-1 clearly decreased Ang II–induced phospho–c-Raf(Ser338).
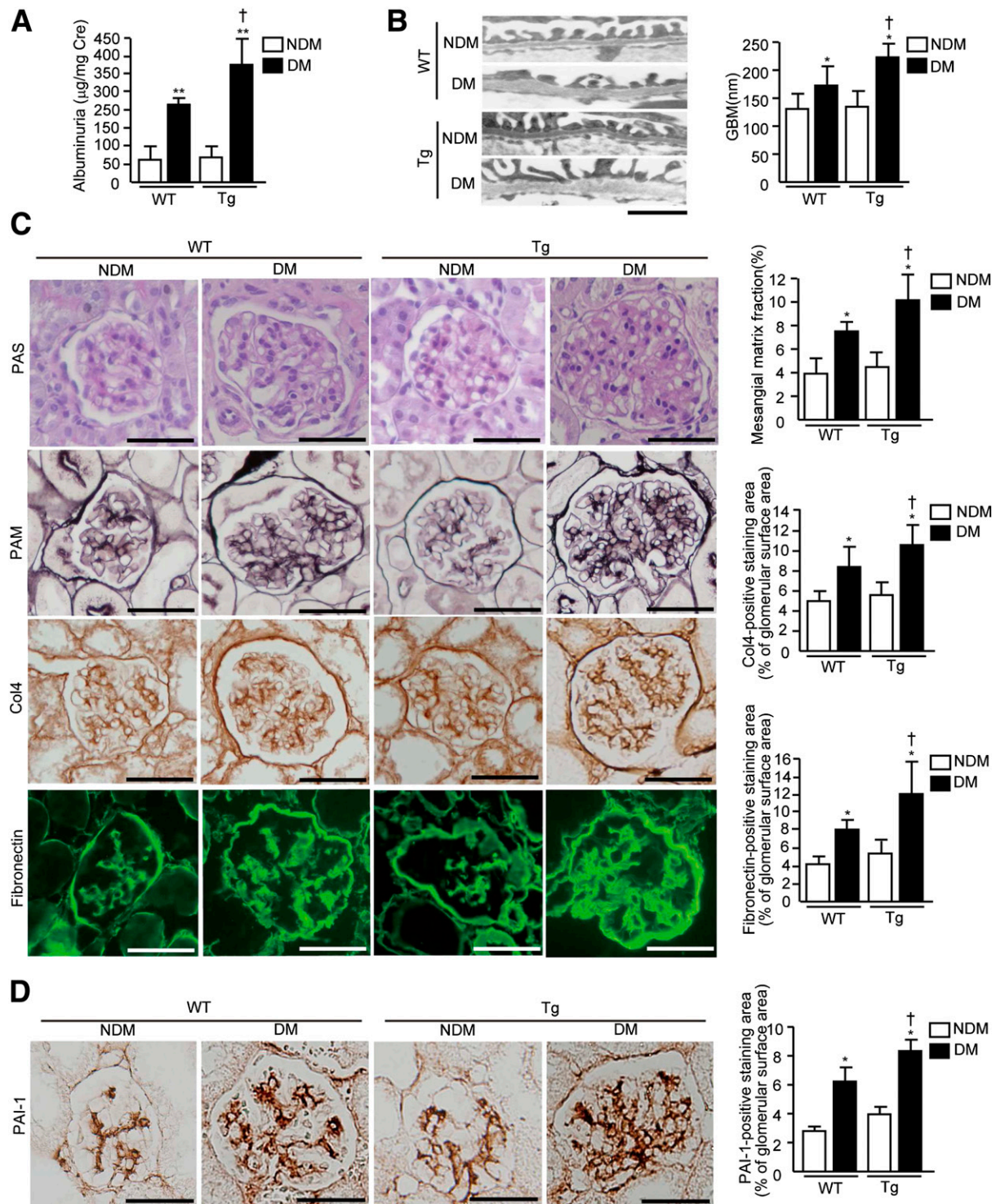
FIG. 3. Functional and histological examinations of diabetic EC-PKCβ2Tg and WT mice. *A*: Albuminuria in mice with STZ-induced diabetes (DM), nondiabetic mice (NDM), WT mice, and EC-PKCβ2Tg mice is shown. $n = 6$ in nondiabetic WT and diabetic WT mice; $n = 7$ in nondiabetic transgenic (Tg) and diabetic transgenic mice. **$P < 0.001$ vs. nondiabetic WT mice. †$P < 0.05$ vs. diabetic WT mice. *B*: Representative views of GBM in each group of mice and quantification of GBM thickness in each group of mice. Bar = 1 μm. $n = 6$ in nondiabetic WT and diabetic WT mice; $n = 7$ in nondiabetic transgenic and diabetic transgenic mice. *$P < 0.05$ vs. nondiabetic WT mice. †$P < 0.05$ vs. diabetic WT mice. *C*: Representative light microscopic appearance of glomeruli (periodic acid–Schiff [PAS] and periodic acid–methenamine-silver [PAM] staining), immunohistochemistry of Col4 and fibronectin, and morphometric analysis of periodic acid–methenamine-silver–, Col4-, and fibronectin-positive staining area. The glomerular periodic acid–methenamine-silver–, Col4-, and fibronectin-positive staining area was measured. Bar = 50 μm. $n = 6$ in nondiabetic WT and diabetic WT mice; $n = 7$ in nondiabetic transgenic and diabetic transgenic mice. *$P < 0.05$ vs. nondiabetic WT mice. †$P < 0.05$ vs. diabetic WT mice. Magnification ×400. *D*: Immunostaining for PAI-1 in each group of mice and analysis of glomerular expression of PAI-1. Bar = 50 μm. $n = 6$ in nondiabetic WT and diabetic WT mice; $n = 7$ in nondiabetic transgenic and diabetic transgenic mice. *$P < 0.05$ vs. nondiabetic WT mice. †$P < 0.05$ vs. diabetic WT mice. Magnification ×400. One of three independently performed experiments is shown. Results are expressed as means ± SD. For all the studies above, comparisons were made between groups using either two-sample and paired *t* tests for two-way comparisons or one-way ANOVA for multiple groups to establish statistically significant differences. (A high-quality digital representation of this figure is available in the online issue.)
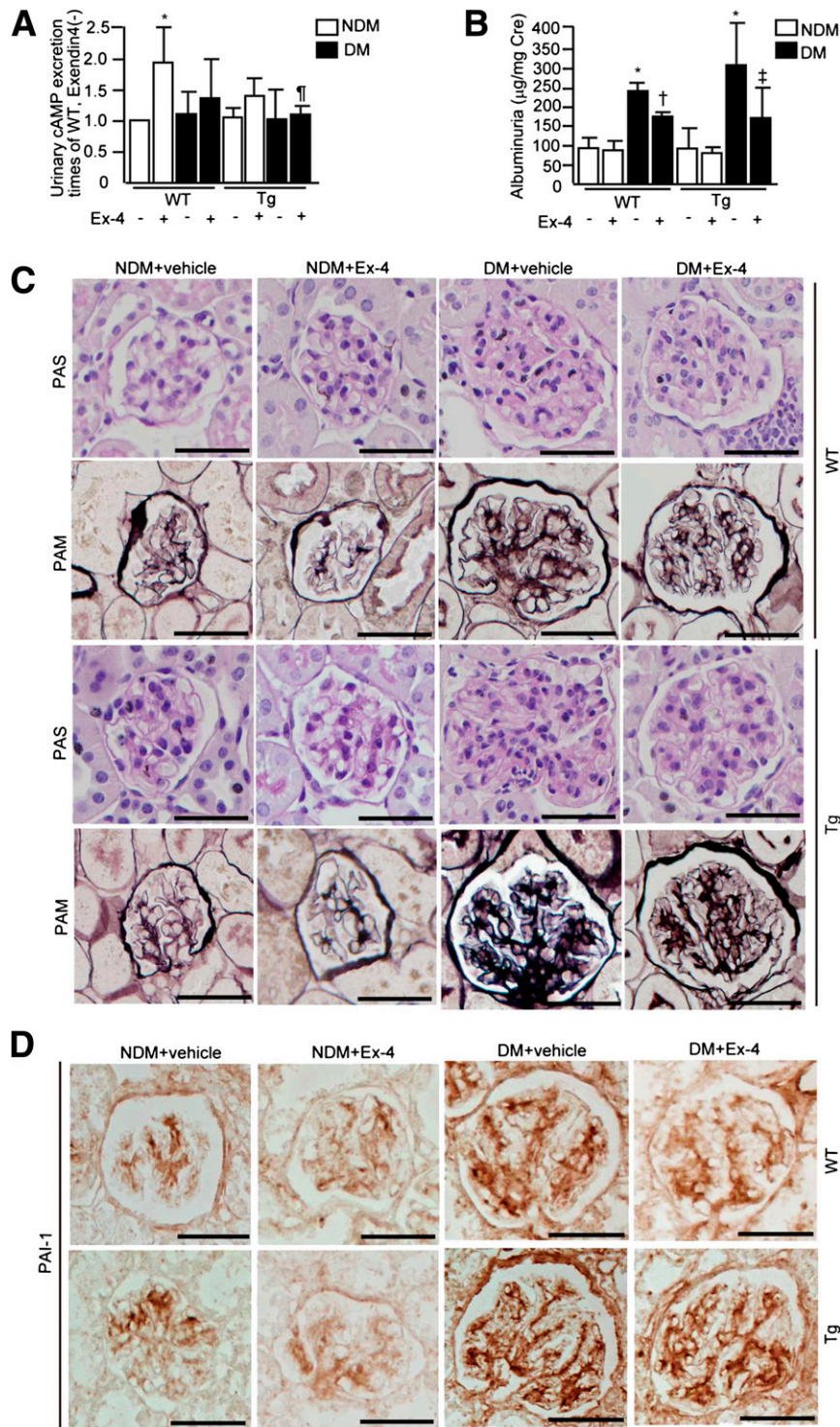
FIG. 4. Effect of exendin-4 (Ex-4) treatment in EC-PKCβ2Tg mice. *A*: Urinary cAMP excretions in each group are shown: mice with STZ-induced diabetes (DM), nondiabetic mice (NDM), WT mice, and EC-PKCβ2Tg mice. *n* = 6 in nondiabetic WT plus vehicle, nondiabetic WT plus exendin-4, diabetic WT plus vehicle, diabetic WT plus exendin-4, nondiabetic transgenic (Tg) plus exendin-4, and diabetic transgenic plus exendin-4; *n* = 7 in nondiabetic transgenic plus vehicle and diabetic transgenic plus vehicle. *P < 0.05 vs. WT/nondiabetic/exendin-4⁻; ¶P < 0.05 vs. WT/nondiabetic/exendin-4⁺. *B*: Albuminuria in each test group is shown. *n* = 6 in nondiabetic WT plus vehicle, nondiabetic WT plus exendin-4, diabetic WT plus vehicle, diabetic WT plus exendin-4, nondiabetic transgenic plus exendin-4, and diabetic transgenic plus exendin-4; *n* = 7 in nondiabetic transgenic plus vehicle and diabetic transgenic plus vehicle. *P < 0.05 vs. WT/nondiabetic/exendin-4⁻; †P < 0.05 vs. WT/diabetic/exendin-4⁻; ‡P < 0.05 vs. transgenic/diabetic/exendin-4⁻. *C*: Representative light microscopic appearance of glomeruli periodic acid–Schiff (PAS) and periodic acid–methenamine-silver (PAM) staining. Bar = 50 μm. *n* = 6 in nondiabetic WT plus vehicle, nondiabetic WT plus exendin-4, diabetic WT plus vehicle, diabetic WT plus exendin-4, nondiabetic transgenic plus exendin-4, and diabetic transgenic plus exendin-4; *n* = 7 in nondiabetic transgenic plus vehicle and diabetic transgenic plus vehicle. Magnification ×400. *D*: Immunostaining for PAI-1 in each group of mice is shown. Bar = 50 μm. *n* = 6 in nondiabetic WT plus vehicle, nondiabetic WT plus exendin-4, diabetic WT plus vehicle, diabetic WT plus exendin-4, nondiabetic transgenic plus exendin-4, and diabetic transgenic plus exendin-4; *n* = 7 in nondiabetic transgenic plus vehicle and diabetic transgenic plus vehicle. Magnification ×400. One of three independently performed experiments is shown. Results are expressed as means ± SD. Comparisons were made between groups using either two-sample and paired *t* tests for two-way comparisons or one-way ANOVA for multiple groups to establish statistically significant differences. (A high-quality digital representation of this figure is available in the online issue.)
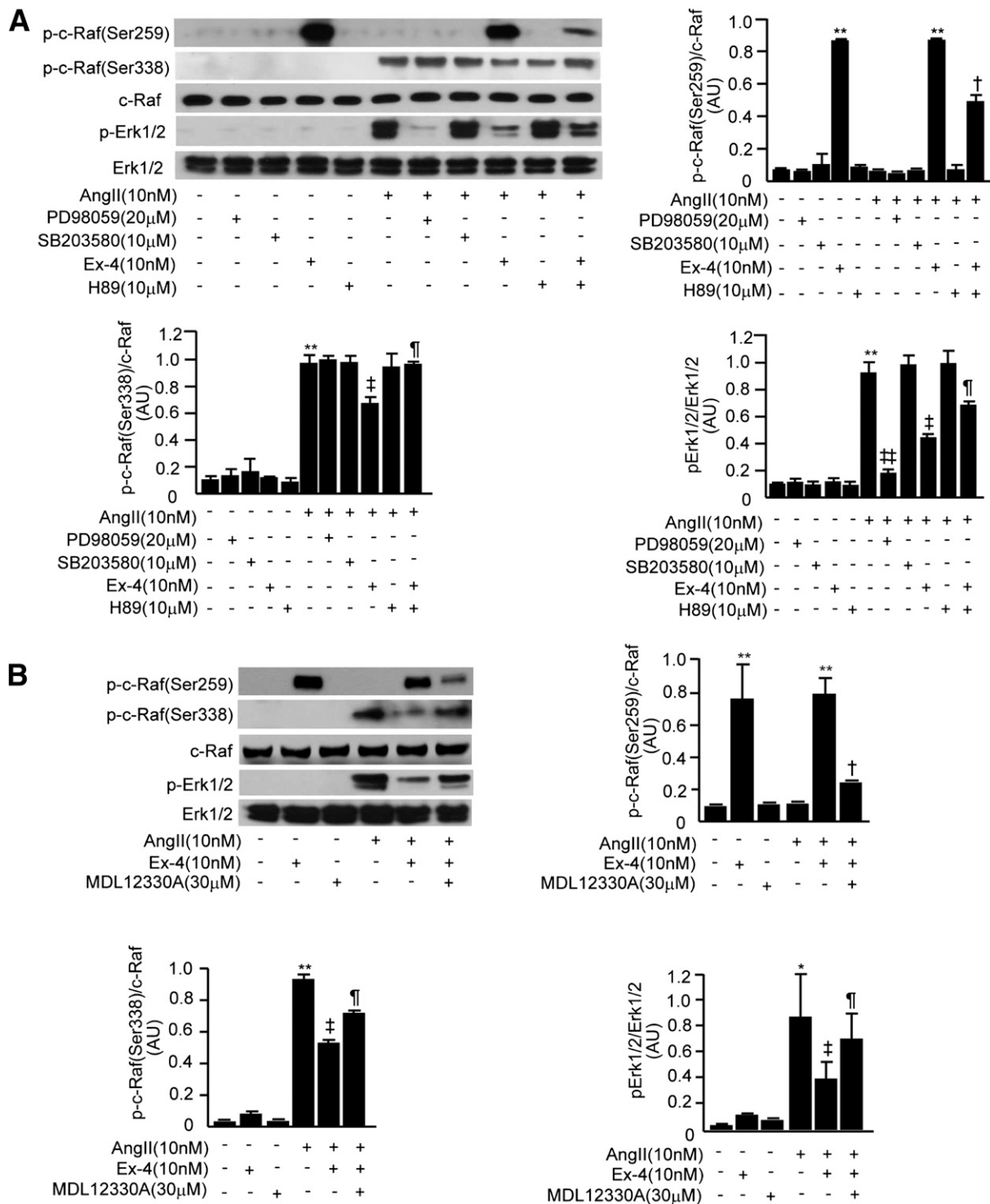
FIG. 5. Exendin-4 (Ex-4) decreased effect of Ang II on Erk1/2/PAI-1 signaling. *A*: Immunoblots of phospho–c-Raf (p-c-Raf)(Ser259), phospho–c-Raf(Ser338), and phospho-Erk1/2 (p-Erk1/2) in RGECs stimulated with Ang II in the presence or absence of PD98059, SB203580, exendin-4, or H89. **$P < 0.001$ vs. Ang II$^-$/PD98059$^-$/SB203580$^-$/exendin-4$^-$/H89$^-$; †$P < 0.05$ vs. Ang II$^-$/PD98059$^-$/SB203580$^-$/exendin-4$^+$/H89$^-$; ‡$P < 0.05$, ‡‡$P < 0.001$ vs. Ang II$^+$/PD98059$^-$/SB203580$^-$/exendin-4$^-$/H89$^-$; ¶$P < 0.05$ vs. Ang II$^+$/PD98059$^-$/SB203580$^-$/exendin-4$^+$/H89$^-$. *B*: Immunoblots of phospho–c-Raf(Ser259), phospho–c-Raf(Ser338), and phospho-Erk1/2 in RGECs stimulated with Ang II (10 nmol/L) in the presence or absence of exendin-4 or MDL12330A. *$P < 0.05$, **$P < 0.001$ vs. Ang II$^-$/exendin-4$^-$/MDL12330A$^-$; †$P < 0.05$ vs. Ang II$^-$/exendin-4$^+$/MDL12330A$^-$; ‡$P < 0.05$ vs. Ang II$^+$/exendin-4$^-$/MDL12330$^-$; ¶$P < 0.05$ vs. Ang II$^+$/exendin-4$^+$/MDL12330$^-$. One of three independently performed experiments is shown. Comparisons were made between groups using either two-sample and paired *t* tests for two-way comparisons or one-way ANOVA for multiple groups to establish statistically significant differences. Results are expressed as means ± SD. AU, arbitrary units.
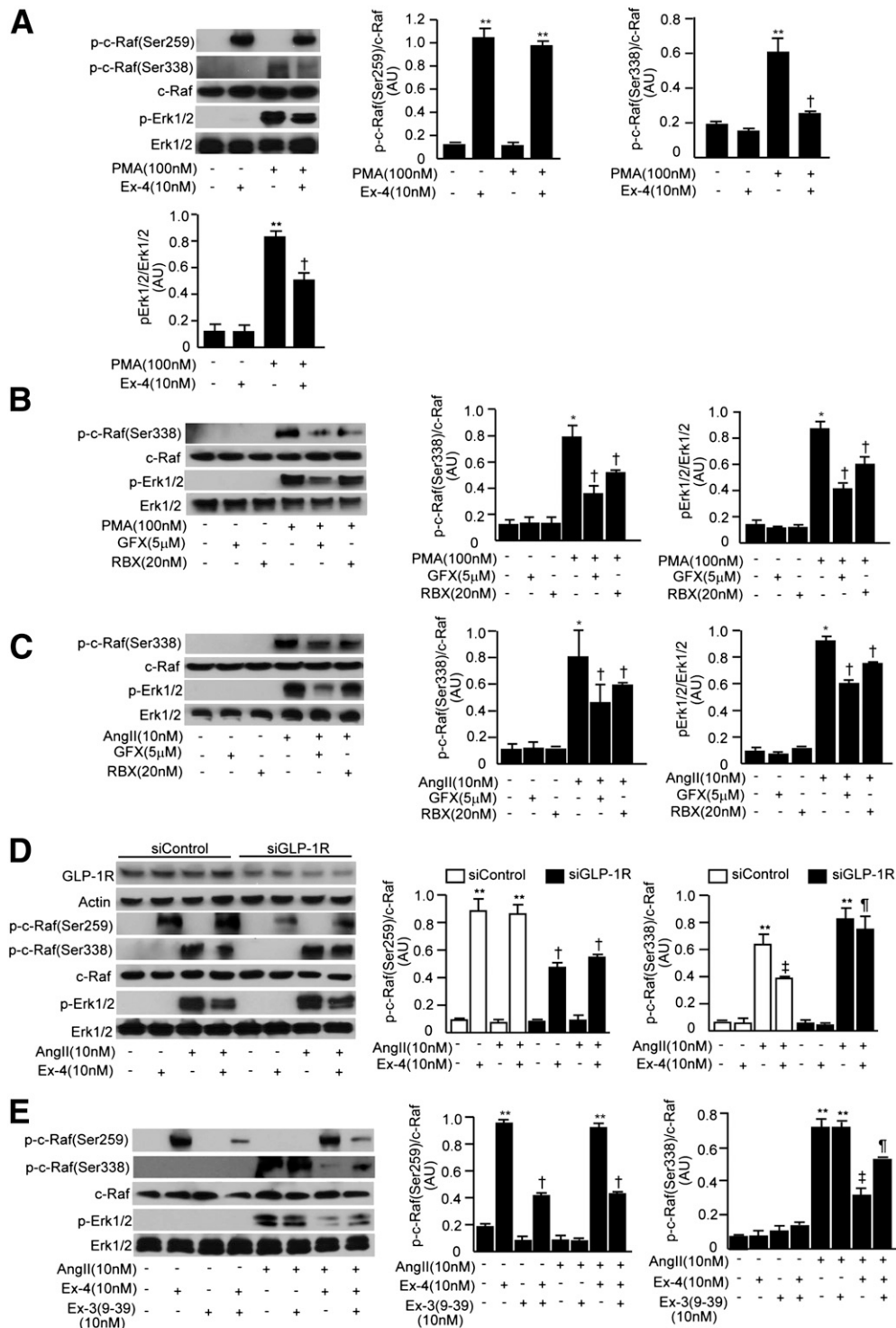
FIG. 6. Effect of PKC activation (PMA), knockdown, or blocking of GLP-1R on exendin-4 (Ex-4)-stimulated inhibition of Ang II on phospho–c-Raf (p-c-Raf)(Ser338), phospho-Erk1/2 (p-Erk1/2), and PAI-1 activity in RGECs. *A*: Immunoblots of phospho–c-Raf(Ser259), phospho–c-Raf(Ser338), and phospho-Erk1/2 in RGECs stimulated with PMA (100 nmol/L) in the presence or absence of exendin-4 are shown. **$P < 0.001$ vs. PMA⁻/exendin-4⁻ and †$P < 0.05$ vs. PMA⁺/exendin-4⁻. *B*: Immunoblots of phospho–c-Raf(Ser338) and phospho-Erk1/2 in RGECs stimulated with PMA in the presence or absence of GFX or RBX. *$P < 0.05$ vs. PMA⁻/GFX⁻/RBX⁻; †$P < 0.05$ vs. PMA⁺/GFX⁻/RBX⁻. *C*: Immunoblots of phospho–c-Raf (Ser338) and phospho-Erk1/2 in RGECs stimulated with Ang II in the presence or absence of GFX or RBX. *$P < 0.05$ vs. Ang II⁻/GFX⁻/RBX⁻; †$P < 0.05$ vs. Ang II⁺/GFX⁻/RBX⁻. *D*: Immunoblots of phospho–c-Raf(Ser259), phospho–c-Raf(Ser338), and phospho-Erk1/2 in RGECs transfected with small interfering GLP-1R or small interfering control, stimulated with Ang II in the presence or absence of exendin-4. **$P < 0.001$ vs. small interfering control/Ang II⁻/exendin-4⁻; †$P < 0.05$ vs. siControl/Ang II⁺/exendin-4⁺; ‡$P < 0.05$ vs. siControl/Ang II⁺/exendin-4⁻; ¶$P < 0.05$ vs. siControl/Ang II⁺/exendin-4⁺. *E*: Immunoblots of phospho–c-Raf(Ser259), phospho–c-Raf(Ser338), and phospho-Erk1/2 in RGECs stimulated with Ang II in the presence or absence of exendin-4 or exendin-3(9-39) [Ex-3(9-39)] are shown. **$P < 0.001$ vs. Ang II⁻/exendin-4⁻/exendin-3(9-39)⁻; †$P < 0.05$ vs. Ang II⁻/exendin-4⁺/exendin-3(9-39)⁻; ‡$P < 0.05$ vs. Ang II⁺/exendin-4⁻/exendin-3(9-39)⁻; ¶$P < 0.05$ vs. Ang II⁺/exendin-4⁺/exendin-3 (9-39)⁻. One of three independently performed experiments is shown. Comparisons were made between groups using either two-sample and paired *t* tests for two-way comparisons or one-way ANOVA for multiple groups to establish statistically significant differences. Results are expressed as means ± SD. AU, arbitrary units.
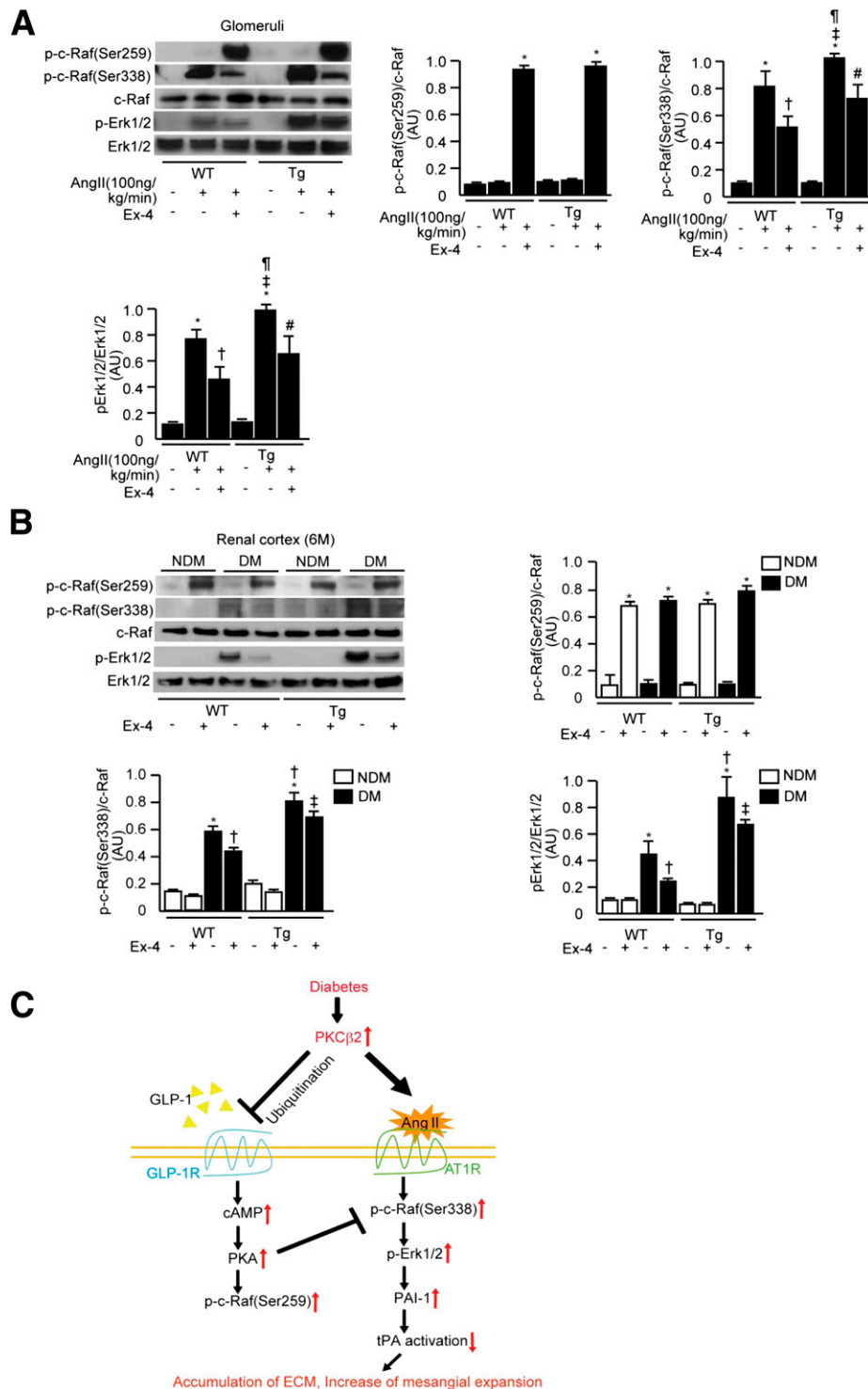
FIG. 7. Exendin-4 (Ex-4) decreased angiotensin II or diabetes-induced increases of phospho–c-Raf (p-c-Raf)(Ser338) in the glomeruli and renal cortex. *A*: Immunoblots of phospho–c-Raf(Ser259), phospho–c-Raf(Ser338), and phospho-Erk1/2 (p-Erk1/2) in the glomeruli. Exendin-4 (1.0 nmol/kg) or diluents were administrated intraperitoneally to mice. After 2-h administration of exendin-4, Ang II (100 ng/kg/3 mL/min) or saline was infused through the jugular vein. After 3-h continuous infusion, glomeruli were corrected. n = 3–5. Tg, transgenic. *P < 0.05 vs. WT/Ang II$^-$/exendin-4$^-$; †P < 0.05 vs. WT/Ang II$^+$/exendin-4$^-$; ‡P < 0.05 vs. transgenic/Ang II$^-$/exendin-4$^-$; ¶P < 0.05 vs. WT/Ang II$^+$/exendin-4$^-$; #P < 0.05 vs. transgenic/Ang II$^+$/exendin-4$^-$. *B*: Immunoblots of phospho–c-Raf(Ser259), phospho–c-Raf(Ser338), and phospho-Erk1/2 in the renal cortex. n = 6 in nondiabetic WT plus vehicle, nondiabetic WT plus exendin-4, diabetic WT plus vehicle, diabetic WT plus exendin-4, nondiabetic transgenic plus exendin-4, and diabetic transgenic plus exendin-4; n = 7 in nondiabetic transgenic plus vehicle and diabetic transgenic plus vehicle. DM, mice with STZ-induced diabetes; NDM, nondiabetic mice. *P < 0.05 vs. WT/nondiabetic/exendin-4$^-$; †P < 0.05 vs. WT/diabetic/exendin-4$^-$; ‡P < 0.05 vs. transgenic/diabetic/exendin-4$^-$. One of three independently performed experiments is shown. Comparisons were made between groups using either two-sample and paired t tests for two-way comparisons or one-way ANOVA for multiple groups to establish statistically significant differences. Results are expressed as means ± SD. *C*: Schematic diagram of the inhibitory effects of PKCβ2 on the protective action of GLP-1 signaling against the effects of Ang II–mediated glomerular pathology. AU, arbitrary units; ECM, extracellular matrix.

Interestingly, Ang II did not inhibit GLP-1 effect on phospho–c-Raf(Ser259). The reduction of c-Raf phosphorylation at Ser338 by GLP-1 caused decreases in phospho-Erk1/2 and PAI-1 in the renal glomeruli.

Diabetes of long duration also inhibited GLP-1–protective action by decreasing GLP-1R via increases in ubiquitination of GLP-1R. However, Zhou et al. (27) reported that high-glucose conditions did not decrease GLP-1R protein expression or increase its ubiquitination in the islet cells after 24 h. Further, Kodera et al. (9) reported that GLP-1R was not decreased in the glomeruli of rats with STZ-induced diabetes after several weeks of disease. However, Park et al. (8) reported that GLP-1R was decreased in the glomeruli of *db/db* mice and exendin-4 treatment ameliorated this decrease. These differences are likely due to using different cell types and mice strains and length of diabetes.

Thus, our results suggest that PKCβ activation induced by hyperglycemia can inhibit GLP-1–protective action and enhance inflammatory effects on the endothelium by at least two signaling pathways. First, our results expand on previous findings and show that PKCβ activation can enhance Ang II effect by phosphorylating c-Raf at Ser338 to activate phospho-Erk1/2 and cause increased production of PAI-1 (28). Second, we found that PKC activation can also inhibit the protective actions of GLP-1 by reducing the expression of its receptors in the endothelial cells. One potential mediator of Ang II adverse effect in endothelial cells is the induction of PAI-1 (7), which may impair fibrinolysis and promote increased extracellular matrix (29,30).

Our study identifies the biochemical mechanisms by which PKC activation can increase the actions of Ang II. The results demonstrate that PKC activation, especially PKCβ, increased phospho–c-Raf(Ser338), which leads to the activation of phospho-Erk1/2. This activation is selective for PKCβ isoform, since RBX, a PKCβ isoform–specific selective inhibitor, inhibited phospho–c-Raf(Ser338). In addition, infusion of Ang II in EC-PKCβ2Tg mice increased phospho–c-Raf(Ser338) to a greater extent than in WT mice both in vivo and in endothelial cells. In parallel with changes in phospho–c-Raf(Ser338), EC-PKCβ2Tg mice exhibited greater expression of PAI-1 than did controls after Ang II infusion. It is interesting to note, however, that endothelial dysfunction induced by the overexpression of PCKβ alone, specifically in the endothelial cells, without the presence of diabetes did not exhibit significant pathology as measured by mesangial matrix expression and PAI-1. Thus, endothelial dysfunction alone without diabetes will only induce minimal albuminuria and extracellular matrix production. Studies using long-duration treatment of Ang II will be needed to correlate changes in phospho–c-Raf and glomerular pathology.

The second new finding shows that diabetes and hyperglycemia via PKCβ activation will blunt the protective actions of GLP-1 by decreasing GLP-1R protein expression in the endothelium. The reduction in GLP-1R is manifested by a decrease in urinary cAMP with infusion of exendin-4 and less reduction in phospho–c-Raf(Ser338)/phospho-Erk1/2 in the glomeruli of EC-PKCβ2Tg mice. However, even with the reduction in GLP-1R, treatment with exendin-4 in vivo was still partially effective to reduce glomerular pathology of both diabetic WT and EC-PKCβ2Tg mice. It is surprising that exendin-4 still had positive effects on the glomerular pathology, although it did not increase urinary cAMP significantly. This could be due to the difficulty of measuring cAMP as a result of degradation in urine that took 24 h to collect and the dilution of samples by the increases of urine volume induced by diabetes. It is also possible that the beneficial effects of exendin-4 could be partially mediated via cAMP-independent pathways. All of the protective actions of exendin-4 occurred without changes in glucose, insulin level, blood pressure, and body weight.

Thus, our study has identified mechanisms by which GLP-1 can induce protective actions on the glomerular endothelial cells by inhibiting the signaling pathway of Ang II at phospho–c-Raf(Ser338) via phospho–c-Raf(Ser259). Further, we have demonstrated, in vivo and in vitro, that hyperglycemia can activate PKCβ isoforms, which enhance Ang II toxic effect in glomerular endothelial cells. These studies suggest that effective therapeutic agents could be designed to enhance GLP-1R on the endothelium, which may prevent glomerular endothelial dysfunction and slow the progression of diabetic nephropathy.

REFERENCES

1. Goldberg RJ, Nakagawa T, Johnson RJ, Thurman JM. The role of endothelial cell injury in thrombotic microangiopathy. Am J Kidney Dis 2010;56:1168–1174
2. Nakagawa T, Tanabe K, Croker BP, et al. Endothelial dysfunction as a potential contributor in diabetic nephropathy. Nat Rev Nephrol 2011;7:36–44
3. Nakagawa T, Sato W, Glushakova O, et al. Diabetic endothelial nitric oxide synthase knockout mice develop advanced diabetic nephropathy. J Am Soc Nephrol 2007;18:539–550
4. Mima A, Ohshiro Y, Kitada M, et al. Glomerular-specific protein kinase C-β-induced insulin receptor substrate-1 dysfunction and insulin resistance in rat models of diabetes and obesity. Kidney Int 2011;79:883–896
5. Naruse K, Rask-Madsen C, Takahara N, et al. Activation of vascular protein kinase C-beta inhibits Akt-dependent endothelial nitric oxide synthase function in obesity-associated insulin resistance. Diabetes 2006;55:691–698
6. Gould CM, Newton AC. The life and death of protein kinase C. Curr Drug Targets 2008;9:614–625
7. Feener EP, Northrup JM, Aiello LP, King GL. Angiotensin II induces plasminogen activator inhibitor-1 and -2 expression in vascular endothelial and smooth muscle cells. J Clin Invest 1995;95:1353–1362

8. Park CW, Kim HW, Ko SH, et al. Long-term treatment of glucagon-like peptide-1 analog exendin-4 ameliorates diabetic nephropathy through improving metabolic anomalies in db/db mice. J Am Soc Nephrol 2007;18: 1227–1238

9. Kodera R, Shikata K, Kataoka HU, et al. Glucagon-like peptide-1 receptor agonist ameliorates renal injury through its anti-inflammatory action without lowering blood glucose level in a rat model of type 1 diabetes. Diabetologia 2011;54:965–978

10. Drucker DJ. The biology of incretin hormones. Cell Metab 2006;3:153–165

11. Bullock BP, Heller RS, Habener JF. Tissue distribution of messenger ribonucleic acid encoding the rat glucagon-like peptide-1 receptor. Endocrinology 1996;137:2968–2978

12. Erdogdu O, Nathanson D, Sjöholm A, Nyström T, Zhang Q. Exendin-4 stimulates proliferation of human coronary artery endothelial cells through eNOS-, PKA- and PI3K/Akt-dependent pathways and requires GLP-1 receptor. Mol Cell Endocrinol 2010;325:26–35

13. Hisatsune H, Matsumura K, Ogawa M, et al. High level of endothelial cell-specific gene expression by a combination of the 5′ flanking region and the 5′ half of the first intron of the VE-cadherin gene. Blood 2005;105:4657–4663

14. Takemoto M, Asker N, Gerhardt H, et al. A new method for large scale isolation of kidney glomeruli from mice. Am J Pathol 2002;161:799–805

15. Siebenlist U, Franzoso G, Brown K. Structure, regulation and function of NF-kappa B. Annu Rev Cell Biol 1994;10:405–455

16. Goodfriend TL, Elliott ME, Catt KJ. Angiotensin receptors and their antagonists. N Engl J Med 1996;334:1649–1654

17. Nicholas SB, Aguiniga E, Ren Y, et al. Plasminogen activator inhibitor-1 deficiency retards diabetic nephropathy. Kidney Int 2005;67:1297–1307

18. Duckworth BC, Cantley LC. Conditional inhibition of the mitogen-activated protein kinase cascade by wortmannin. Dependence on signal strength. J Biol Chem 1997;272:27665–27670

19. Bentires-Alj M, Kontaridis MI, Neel BG. Stops along the RAS pathway in human genetic disease. Nat Med 2006;12:283–285

20. Sharma K, Ix JH, Mathew AV, et al. Pirfenidone for diabetic nephropathy. J Am Soc Nephrol 2011;22:1144–1151

21. Jiang ZY, Lin YW, Clemont A, et al. Characterization of selective resistance to insulin signaling in the vasculature of obese Zucker (fa/fa) rats. J Clin Invest 1999;104:447–457

22. Hirata K, Kume S, Araki S, et al. Exendin-4 has an anti-hypertensive effect in salt-sensitive mice model. Biochem Biophys Res Commun 2009;380:44–49

23. Cook SJ, McCormick F. Inhibition by cAMP of Ras-dependent activation of Raf. Science 1993;262:1069–1072

24. Dhillon AS, Pollock C, Steen H, Shaw PE, Mischak H, Kolch W. Cyclic AMP-dependent kinase regulates Raf-1 kinase mainly by phosphorylation of serine 259. Mol Cell Biol 2002;22:3237–3246

25. Hagiwara M, Brindle P, Harootunian A, et al. Coupling of hormonal stimulation and transcription via the cyclic AMP-responsive factor CREB is rate limited by nuclear entry of protein kinase A. Mol Cell Biol 1993;13: 4852–4859

26. Doucas V, Shi Y, Miyamoto S, West A, Verma I, Evans RM. Cytoplasmic catalytic subunit of protein kinase A mediates cross-repression by NF-kappa B and the glucocorticoid receptor. Proc Natl Acad Sci USA 2000; 97:11893–11898

27. Zhou J, Livak MF, Bernier M, et al. Ubiquitination is involved in glucose-mediated downregulation of GIP receptors in islets. Am J Physiol Endocrinol Metab 2007;293:E538–E547

28. Koyanagi T, Wong LY, Inagaki K, Petrauskene OV, Mochly-Rosen D. Alteration of gene expression during progression of hypertension-induced cardiac dysfunction in rats. Am J Physiol Heart Circ Physiol 2008;295: H220–H226

29. Tofler GH, Massaro J, Levy D, et al. Relation of the prothrombotic state to increasing age (from the Framingham Offspring Study). Am J Cardiol 2005; 96:1280–1283

30. Paueksakon P, Revelo MP, Ma LJ, Marcantoni C, Fogo AB. Microangiopathic injury and augmented PAI-1 in human diabetic nephropathy. Kidney Int 2002;61:2142–2148